

Thermal Shock Resistance of Silicon Nitrides Using an Indentation–Quench Test

Seung Kun Lee,^{*,†} James D. Moretti,[‡] and Michael J. Readey^{*}

Advanced Materials Technology, Caterpillar Inc., Peoria, Illinois 61656

Brian R. Lawn^{*}

Material Science and Engineering Laboratory, National Institute of Standards and Technology, Gaithersburg, Maryland 20899

Thermal shock resistance of silicon nitrides is investigated using an indentation–quench method. Four commercially available silicon nitrides with different microstructures are investigated. The extension of Vickers radial cracks is measured as a function of quenching temperature for each material, up to the critical temperature for failure. An indentation fracture mechanics analysis is used to account for the crack responses, with due allowance for *R*-curve behavior. The analysis confirms the important role of microstructure in thermal shock resistance.

I. Introduction

THERMAL shock can limit performance in many ceramic applications. Formal fracture mechanics analyses of thermal shock resistance were pioneered by Hasselman,^{1,2} implicitly for simple ceramics with single-valued toughness. Swain³ extended the fracture mechanics to ceramics with *R*-curves. In conventional testing thermal shock resistance is quantified by measuring the residual strength of polished specimens after quenching. A more economical approach is to measure the extension of indentation precracks as a function of quench temperature,^{4–6} where several data points may be taken from one specimen surface at each quench temperature.

Silicon nitride has been in the forefront of modern ceramic applications as a durable high-temperature material with good thermal shock resistance, as well as low susceptibility to fracture, wear, and fatigue. Underlying its high performance are toughness and hardness properties. These properties can be controlled by tailoring the microstructure. Most prominent has been the production of high-toughness silicon nitrides with elongate grains via additives and heat treatments,^{7–11} leading to *R*-curve behavior associated with crack bridging and thence enhanced thermal shock resistance.³

In this paper the relative thermal shock resistance of four commercially available silicon nitrides is investigated using an indentation–quench method. Vickers indentations are made on rectangular bars, which are then heated to predetermined temperatures and quenched into water. Crack extensions from the

indentations are measured as a function of quench temperature differential, and the critical temperatures for spontaneous crack growth (failure) thereby determined for each material. A fracture mechanics analysis taking into account measured *R*-curve functions is used to account for the data trends.

II. Experimental Procedure

Four commercially available silicon nitrides with different microstructures were examined. Figure 1 shows microstructures of each material, and Table I lists thermomechanical properties. All microstructures are bimodal with a mixture of fine, equiaxed grains and coarse, elongate grains, and with bonding grain boundary phase: (a) CFI3208 (Ceramic for Industry, Roedental, Germany) has a relatively fine microstructure with a small percentage of elongate grains; (b) SN235P (Kyocera, Vancouver, WA) is coarser with a higher percentage of elongate grains; (c) GS44 (Honeywell, Torrance, CA) is coarser still with an even higher percentage of elongate grains; (d) AS800 (Honeywell, Torrance, CA) consists mostly of coarse elongate grains. Note an apparent correlation between the grain size in these microstructures and the (long-crack) toughness values listed in Table I.

Specimens were prepared as bars 50 mm × 4 mm × 3 mm, surface-finished with 1 μm diamond paste. Vickers indentations with well-defined radial cracks^{12,13} were made at prescribed loads in the specimen top surfaces. A minimum of eight noninteracting indentations at any prescribed load were placed along a center line on any one surface, with the radial cracks aligned parallel to both specimen edges.

The indented specimens were heated to temperatures up to 1000°C in laboratory atmosphere. The temperatures were held at a specified maximum for 20 min, after which the specimens were quenched in distilled water at room temperature. Final radial crack lengths were then measured with an optical microscope in Nomarski interference contrast. This procedure was repeated at increasing quench temperatures, up to the critical value at which one radial crack became unstable and the specimen failed.

Four-point flexure tests were conducted on unquenched bars containing a single centered Vickers indentation, loading rate 30 MPa·s⁻¹, for toughness evaluation.¹⁴

III. Fracture Mechanics

Thermal shock treatments at quench temperature differentials ΔT induce maximum tensile stresses σ in the specimen surfaces:^{1,2}

$$\sigma = BE\alpha\Delta T/(1 - \nu) = A\Delta T \quad (1)$$

where α is the thermal expansion coefficient, E Young's modulus, ν Poisson's ratio, B a dimensionless constant (value ≤ 1), and $A =$

P. F. Becher—contributing editor

Manuscript No. 187648. Received June 27, 2001; approved October 13, 2001.

^{*}Member, American Ceramic Society.

This work was supported by the U.S. Department of Energy under Contract No. DE-FC05-97OR22579.

[†]Now at LTD Ceramics Inc., Newark, California 94560.

[‡]Intern student from Alfred University, Alfred, New York.

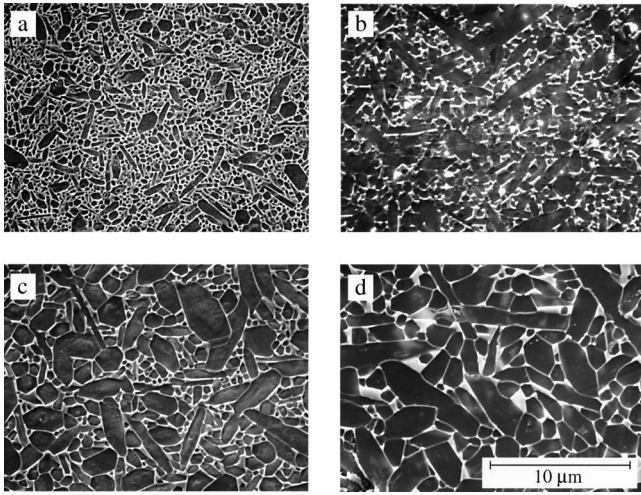


Fig. 1. SEM micrographs of silicon nitrides: (a) CFI3208, (b) SN235P, (c) GS44, and (d) AS800. Dark regions indicate silicon nitride grains, white regions indicate grain boundary phases. Surfaces plasma-etched to reveal grain boundaries.

$BE\alpha/(1 - \nu)$ a thermomechanical quantity. B is dependent on several factors, notably the Biot modulus $\beta = r_0h/k$, where r_0 is a characteristic specimen dimension, h the heat transfer coefficient, and k the thermal conductivity. We take the quantity A to be comparable for most silicon nitrides used in this study (Table I).

Consider a specimen containing a Vickers indentation flaw in the center top surface, induced at load P and with cracks of radial dimension c . Suppose the material to have a monotonically increasing crack-size-dependent toughness $K_R(c)$ (R -curve). The applied K -field acting on the indentation flaw subjected to thermal stress σ is³

$$K_A(c) = \psi\sigma c^{1/2} + \chi P/c^{3/2} = K_R(c) \quad (2)$$

where ψ is a crack geometry constant and χ is a coefficient associated with residual elastic-plastic stresses around the Vickers impression.^{12,15} The equality $K_A(c) = K_R(c)$ expresses the condition for the crack to extend in equilibrium. This extension is initially stable with increasing ΔT , until instability is attained at $c = c_*$ and $\Delta T = \Delta T_*$ (failure). Inserting $\sigma = A\Delta T$ from Eq. (1) into Eq. (2) yields

$$\Delta T = (K_R/\psi A c^{1/2})[1 - \chi P/K_R c^{3/2}] \quad (3)$$

from which the thermal shock function $c(\Delta T)$, and thence the critical quench temperature differential ΔT_* , may be obtained, once $K_R(c)$ is determined.

IV. Results

Micrographic examination of thermally shocked specimens with Vickers indentations showed a reproducible, well-defined radial crack pattern. These cracks increased monotonically in size

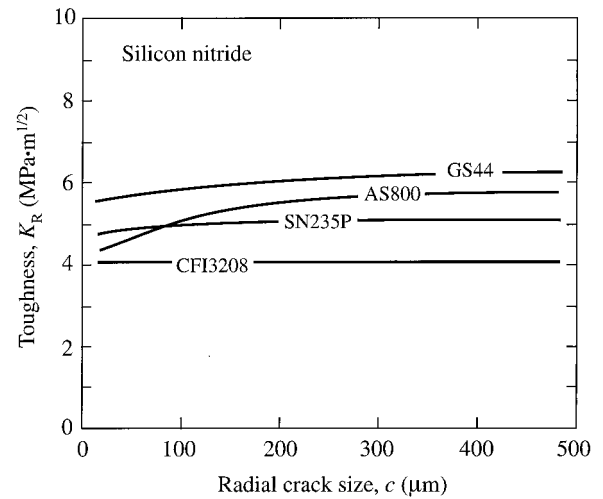


Fig. 2. $K_R(c)$ curves for silicon nitrides, deconvoluted from Vickers indentation-strength data.

c with increasing ΔT , but always reached instability at $\Delta T = \Delta T_*$ first in the longitudinal direction (i.e., parallel to the long specimen edge). This indicates a slightly higher tension in the transverse direction, consistent with some edge effect in the thermal transfer process (via r_0 in the Biot coefficient in Eq. (1)).

Figure 2 plots toughness curves for all silicon nitrides, here deconvoluted directly from indentation-strength $\sigma_F(P)$ data.¹⁴ Only CFI3208 showed classical $\sigma_F \propto P^{-1/3}$ dependence for materials with single-valued toughness^{12,13}—departures from this dependence for the other materials are reflected as K_R -curves in Fig. 2.

Indentation-quench tests on CFI3208 were thereby made to determine controlling parameters in Eq. (3). Figure 3 plots $c(\Delta T)$ for longitudinal radial cracks at four indentation loads. Three distinct stages characterize the crack evolution: (i) an initial stage of zero extension; (ii) a subsequent stage of precursor stable extension; and (iii) a final stage of unstable extension to the longitudinal specimen edges. The precursor growth reflects the stabilizing influence of residual elastic-plastic indentation stresses in the fracture mechanics,^{12,13} and signals impending failure. The initial passive stage is attributable to some postindentation, pre-quench relaxation of these residual contact stresses.¹⁶ The final, unstable stage determines the failure condition. The CFI3208 data in Fig. 3 may be represented by Eq. (3) with $K_R = K_0 = \text{constant}$. Simultaneous best fits to the data in Fig. 3 and the CFI3208 indentation-strength data yielded $A = 0.52 \text{ MPa}\cdot\text{C}^{-1}$, $K_0/\psi = 5.14 \text{ MPa}\cdot\text{m}^{1/2}$, and $K_0/\chi = 100 \text{ MPa}\cdot\text{m}^{1/2}$. Solid curves regenerated in Fig. 3 from Eq. (3) using these parameters follow essential data trends. Taking $\psi = 0.77$ for the material-independent crack geometry constant from a previous parameter evaluation^{14,17} yields $K_0 = 4.0 \text{ MPa}\cdot\text{m}^{1/2}$ for CFI3208 silicon nitride, thence $\chi = 0.040$. Strictly, $\chi \propto (E/H)^{1/2}$, where E/H is the ratio of Young's

Table I. Properties of Silicon Nitride Used in This Study

Silicon nitride	CFI3208	SN235P	GS44	AS800
Grain dimensions (μm) [†]	0.2×1.5	0.8×4.0	0.9×5.5	1.8×7.5
Strength (MPa)	730	790	959	707
Toughness ($\text{MPa}\cdot\text{m}^{1/2}$)	4.0	5.2 [‡]	6.2 [‡]	5.8 [‡]
Hardness (GPa)	15.2	15.5	15.2	14.8
Young's modulus (GPa)	310	300	310	305
Poisson's ratio	0.28	0.28	0.28	0.28
Thermal expansion coeff (10^{-6} K^{-1})	3.2	3.5	3.5	3.7
Thermal conductivity ($\text{W}\cdot\text{m}^{-1}\cdot\text{K}^{-1}$)	30	31	25	41

[†]Elongate grains. [‡] R -curve, long-crack toughness.

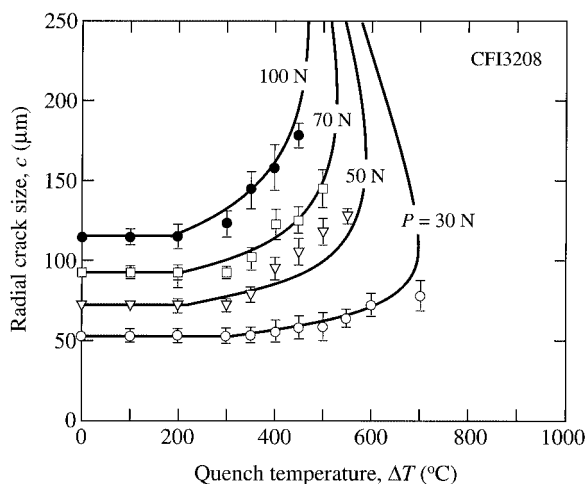


Fig. 3. Effect of indentation load P on radial crack evolution $c(\Delta T)$ for CFI3208 silicon nitride. Symbols are means and standard deviations of experimental data points for a minimum eight indentations per point, curves are fits to Eq. (3). Note reduction in critical quench temperature differential with increasing P .

modulus to hardness¹⁵—however, since E/H does not vary strongly in Table I, we assume it to have the same value for all of the silicon nitrides.

Plots of $c(\Delta T)$ for the four silicon nitrides are shown in Fig. 4, for a fixed indentation load $P = 70$ N. The solid curves are predictions from Eq. (3), using A , ψ , and χ as evaluated above. The curves fit most of the data within the standard deviation error bars, except for the AS800 material, where the experimental thermal shock resistance is higher than predicted. The intermaterial trends in Fig. 4 reflect the relative toughness values in Fig. 2 in the crack size range 75–150 μm .

V. Discussion

The thermal shock resistance of four commercially available silicon nitrides has been evaluated using an indentation–quench

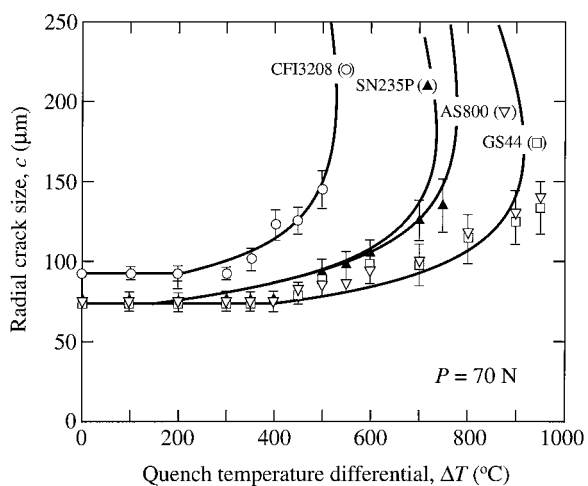


Fig. 4. Longitudinal radial crack evolution $c(\Delta T)$ for different silicon nitrides, for indentations at $P = 70$ N. Symbols are means and standard deviations of experimental data points for a minimum eight indentations per point, curves are predictions from Eq. (3).

method. The method monitors the extension of Vickers precracks as a function of quench temperature differential ΔT . A basic fracture mechanics description, with allowance for R -curve behavior in the material toughness characteristics, accounts for the main features in the crack evolution to failure, notwithstanding some quantitative discrepancies for one material (AS800). Given a suitable parameter calibration on one, reference silicon nitride, we were able to predict the thermal shock resistance of the other silicon nitrides.

The results in Fig. 3 confirm an expected effect of initial flaw size on thermal shock resistance—larger surface flaws (higher indentation loads) result in a lower ΔT_* . Figure 4 demonstrates that ΔT_* is enhanced by coarsening and elongating the silicon nitride microstructures, via the influence on toughness and R -curve behavior. In practice, this advantage has to be balanced against a greater susceptibility of tougher silicon nitrides to fatigue and wear.¹⁸

The indentation–strength test method provides certain experimental advantages. The number of specimens that need to be studied is relatively small compared to more conventional test methods. Some assumptions in the fracture mechanics, specifically that the constant A is material-, geometry-, and temperature-independent, may need closer scrutiny in any more detailed analysis or in intercomparisons between unlike material types and different specimen geometries.

References

- D. P. H. Hasselman, "Unified Theory of Thermal Shock Fracture Initiation," *J. Am. Ceram. Soc.*, **52**, 600 (1969).
- W. D. Kingery, H. K. Bowen, and D. R. Uhlmann, *Introduction to Ceramics*; Ch. 16. Wiley, New York, 1976.
- M. V. Swain, "R-Curve Behavior and Thermal Shock Resistance of Ceramics," *J. Am. Ceram. Soc.*, **73** [3] 621–28 (1990).
- D. P. H. Hasselman, E. P. Chen, and P. A. Urlick, "Prediction of the Thermal Fatigue Resistance of Indented Glass Rods," *Am. Ceram. Soc. Bull.*, **57** [2] 190–92 (1978).
- F. Osterstock, "Contact Damage Submitted to Thermal Shock: A Method to Evaluate and Simulate Thermal Shock Resistance of Brittle Materials," *Mater. Sci. Eng.*, **A168**, 41–44 (1993).
- T. Anderson and D. J. Rowcliffe, "Indentation Thermal Shock Resistance for Ceramics," *J. Am. Ceram. Soc.*, **79** [6] 605–10 (1996).
- F. F. Lange, "Relation Between Strength, Fracture Energy, and Microstructure of Hot-Pressed Si_3N_4 ," *J. Am. Ceram. Soc.*, **59** [10] 518–22 (1973).
- C.-W. Li and J. Yamanis, "Super-Tough Silicon Nitride with R-Curve Behavior," *Ceram. Eng. Sci. Proc.*, **10** [7–8] 632–45 (1989).
- C.-W. Li, D.-J. Lee, and S.-C. Lui, "R-Curve Behavior and Strength of In-Situ-Reinforced Silicon Nitride with Different Microstructures," *J. Am. Ceram. Soc.*, **75** [7] 1777–85 (1992).
- C.-W. Li, S.-C. Lui, and J. Goldacker, "Relation Between Strength, Microstructure, and Grain-Bridging Characteristics in In-Situ-Reinforced Silicon Nitride," *J. Am. Ceram. Soc.*, **78** [2] 449–59 (1995).
- S. K. Lee, K. S. Lee, B. R. Lawn, and D. K. Kim, "Effect of Starting Powder on Damage Resistance of Silicon Nitrides," *J. Am. Ceram. Soc.*, **81** [8] 2061–70 (1998).
- D. B. Marshall and B. R. Lawn, "Residual Stress Effects in Sharp-Contact Cracking: I, Indentation Fracture Mechanics," *J. Mater. Sci.*, **14** [8] 2001–12 (1979).
- D. B. Marshall, B. R. Lawn, and P. Chantikul, "Residual Stress Effects in Sharp-Contact Cracking: II, Strength Degradation," *J. Mater. Sci.*, **14** [9] 2225–35 (1979).
- L. M. Braun, S. J. Bennison, and B. R. Lawn, "Objective Evaluation of Short-Crack Toughness-Curves Using Indentation Flaws: Case Study on Alumina-Based Ceramics," *J. Am. Ceram. Soc.*, **75** [11] 3049–57 (1992).
- B. R. Lawn, A. G. Evans, and D. B. Marshall, "Elastic/Plastic Indentation Damage in Ceramics: The Median/Radial Crack System," *J. Am. Ceram. Soc.*, **63** [9–10] 574–81 (1980).
- B. R. Lawn, D. B. Marshall, and P. Chantikul, "Mechanics of Strength Degrading Flaws in Silicon," *J. Mater. Sci.*, **16** [7] 1769–75 (1981).
- S. K. Lee, S. Wuttiphon, and B. R. Lawn, "Role of Microstructure in Hertzian Contact Damage in Silicon Nitride: I, Mechanical Characterization," *J. Am. Ceram. Soc.*, **80** [9] 2367–81 (1997).
- S. K. Lee and B. R. Lawn, "Contact Fatigue in Silicon Nitride," *J. Am. Ceram. Soc.*, **82** [5] 1281–88 (1999). □